Reduction of neutron-induced background in KOTO

2017 J. Phys.: Conf. Ser. 800 012025

(http://iopscience.iop.org/1742-6596/800/1/012025)

IOP Conf. Series: Journal of Physics: Conf. Series **800** (2017) 012025 doi:10.1088/1742-6596/800/1/012025

Reduction of neutron-induced background in KOTO

Kota Nakagiri for the KOTO collaboration

Department of Physics, Faculty of Science, Kyoto University Kitashirakawa Oiwake-cho, Sakyo-ku, Kyoto, 606-8502, Japan

E-mail: n-kota@scphys.kyoto-u.ac.jp

Abstract.

The KOTO experiment aims to study the $K_L \to \pi^0\nu\overline{\nu}$ decay at J-PARC. In order to identify the signal, we measure two photons from a π^0 decay with an electromagnetic calorimeter consisting of undoped CsI crystals, and ensure that there are no other particles with hermetic veto counters. In the analysis of data taken in 2013, the neutron-induced background, which was caused by a beam-halo neutron hitting the calorimeter was dominant. The neutron makes a primary hadronic shower and a secondary neutron emitted from the shower makes a secondary shower after traveling inside the calorimeter. If these two shower clusters are observed in the calorimeter without any hits in veto detectors, it can mimic a signal event. We developed new methods to suppress this background, such as neutron-photon discrimination methods using cluster shape and pulse shape. We obtained $(3.8^{+2.4}_{-1.1}) \times 10^4$ reduction power for the neutron-induced background.

1. Introduction

1.1. $K_L \to \pi^0\nu\overline{\nu}$ decay

The $K_L \to \pi^0\nu\overline{\nu}$ decay is a CP-violating rare decay. This decay is a flavor changing neutral current process and is caused via loops. The branching ratio of this decay is predicted to be $(3.00 \pm 0.30) \times 10^{-11}$ in the Standard Model [1] with the theoretical uncertainty of 1–2%. It enables us to observe effects from new physics beyond the Standard Model which enhance the branching ratio.

1.2. KOTO experiment

The KOTO experiment aims to study the $K_L \to \pi^0\nu\overline{\nu}$ decay at the Japan Proton Accelerator Research Complex (J-PARC). In the KOTO experiment, signal candidates are identified by "two photons and nothing else." We measure two photons from a π^0 decay with an electromagnetic calorimeter consisting of undoped CsI crystals, and ensure that there are no other particles with hermetic veto counters (Figure 1). We also use π^0 kinematical information, which is reconstructed from energy and position information of two photon clusters on the CsI calorimeter for the identification. We set the signal region in a scatter plot of π^0 transverse momentum (P_t) versus π^0 decay Z vertex.

In 2013, we performed the first physics run and achieved single event sensitivity of 1.29×10^{-8} with only four days of data taking [2], which is equivalent to the sensitivity achieved by the KEK E391a experiment [3]. One event was observed, and it was consistent with the estimated number of background events. We found the mechanism of "neutron-induced background", which is explained in section 2, was a dominant background in the analysis.

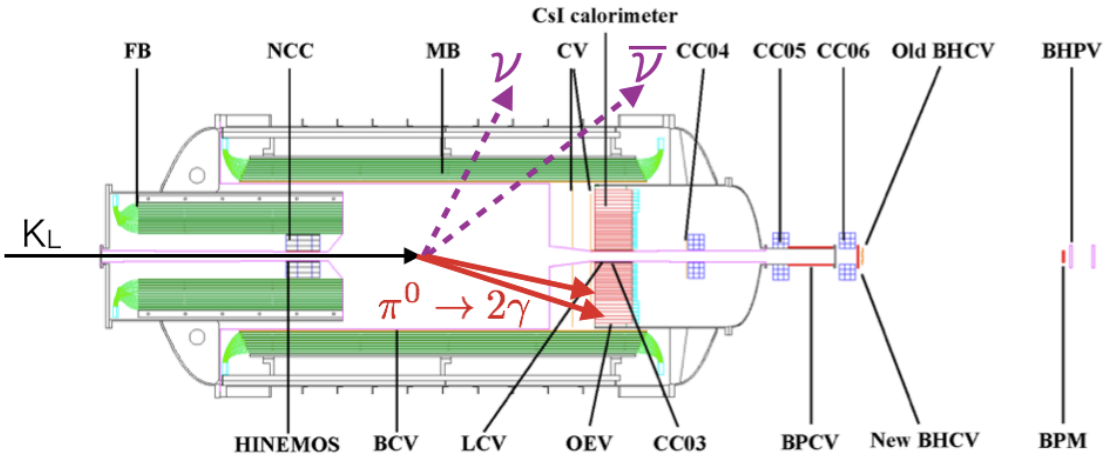

Figure 1. Schematic cross-sectional view of the KOTO detector.

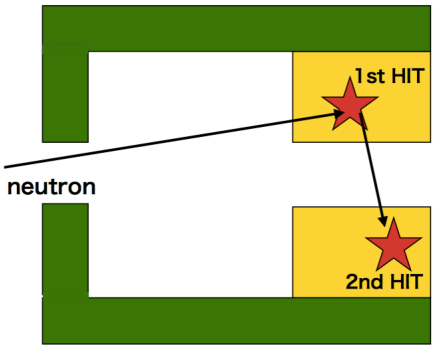

Figure 2. Mechanism of neutron-induced background. An incident primary neutron has hadronic interactions and makes a primary shower. An emitted secondary neutron from the shower makes another shower after traveling in the calorimeter.

We took data in 2015 and accumulated 20 times more data than that in the 2013 run. We also performed a special run to collect neutron samples, which is described in section 3.1.

2. Neutron-induced background

In the 2013 analysis, we found that beam-halo neutrons hitting the CsI calorimeter are the dominant source of our background. A beam-halo neutron hits the CsI calorimeter and forms a primary hadronic shower. In the interactions, a secondary neutron can be emitted and it produces a secondary shower after traveling inside the calorimeter (Figure 2). These two shower clusters can be observed without hits in any veto detectors. If such an event is reconstructed in the signal box, it will be a background. In 2013, the estimated number of this "neutron-induced background" was 0.18 out of the total expected background events of 0.34.

3. Methods to suppress neutron-induced background

We have developed several methods to suppress the neutron-induced background. The key of the background reduction is to distinguish a photon cluster from a neutron cluster using calorimeter hit information. The methods named "Shape χ^2," "Cluster Shape Discrimination," and "Pulse Shape Likelihood" that we developed will be explained in this paper. The first two use cluster shape information, and the last one uses waveform information from the hits in the calorimeter. The Shape χ^2 method has been used in the 2013 analysis, and the Cluster Shape Discrimination and the Pulse Shape Likelihood are newly developed after that.

3.1. Special run to collect neutron samples : Al target run

Evaluation of the neutron-induced background by means of simulation is difficult due to uncertainties in incident halo-neutron flux, energy, and their interactions. An "Al target run" was performed during the beam time to collect neutron-rich data as control samples. These data were used to evaluate the reduction power of neutron-induced background in each cut.

In the Al target run, a 10-mm-thick aluminum plate was inserted into the beam core at the upstream of the KOTO detector to scatter beam-core neutrons. Scattered neutrons hit the CsI calorimeter and made the events similar to the neutron-induced background.

3.2. Shape χ^2 cut

The dimensions of the cross section of our CsI crystals are 25 mm × 25 mm for this inner 1.2×1.2 m^2 region and 50 mm × 50 mm for the outer region, respectively. This small size of crystal gives us the information of two-dimensional shower shape. The Shape χ^2 method compares the observed energy deposit in each crystal in a cluster with its expected energy derived from a simulation. We qualify the validity of shower shape with the χ^2 defined as follows with an assumption that the cluster is made by a photon :

$$\chi^2 = \frac{1}{N} \sum_{i}^{27\times27 \text{ region}} \left(\frac{e_i/E_{inc} - \mu_i}{\sigma_i} \right)^2, \tag{1}$$

where E_{inc} is the measured photon energy, e_i is the measured deposit energy in i-th crystal, μ_i and σ_i are the expected mean and standard deviation of e_i/E_{inc} respectively, obtained from a simulation with photon. The summation is taken over 27×27 crystals around the cluster center. We reject the event if a cluster has larger Shape χ^2 value than a pre-defined threshold. The background reduction of 300 is obtained with 80% signal acceptance, which is consistent with the 2013 analysis.

3.3. Cluster Shape Discrimination cut

Cluster Shape Discrimination also uses the cluster shape information, and uses a neural net based on several variables from a cluster shape. The main difference from the Shape χ^2 is that it uses the time difference among the crystals in a cluster. Figure 3 shows the energy and time difference distributions derived from a simulation. We can obtain expected time distribution in the cluster and compare it with data. Figure 4 shows distributions of the neural net output. The black histogram shows photon cluster samples and the red histogram shows neutron cluster samples. The background reduction of 1500 is obtained with 90% signal acceptance.

3.4. Pulse Shape Likelihood cut

Pulse Shape Likelihood method uses pulse shape information. The waveforms of all channels of the calorimeter were recorded by using 125 MHz ADC modules with a Gaussian filter in the KOTO experiment. This method extracts the information of the waveform by fitting with an asymmetric gaussian as follows.

$$A(t) = |A| exp\left(-\frac{(t-t_0)^2}{2\sigma(t)^2} \right), \qquad \sigma(t) = \sigma_0 + a(t-t_0). \tag{2}$$

In this function, the σ depends on the distance from the mean (t_0). Due to the difference of dE/dx of electromagnetic showers and hadronic showers, scintillating mechanism may be different and appears in the waveform difference. In the neutron case, a hadronic shower may have a larger tail component. It makes the "σ_0" and "a" parameters in the fitting function larger. By using such information, the likelihood ratio is calculated to determine which is more

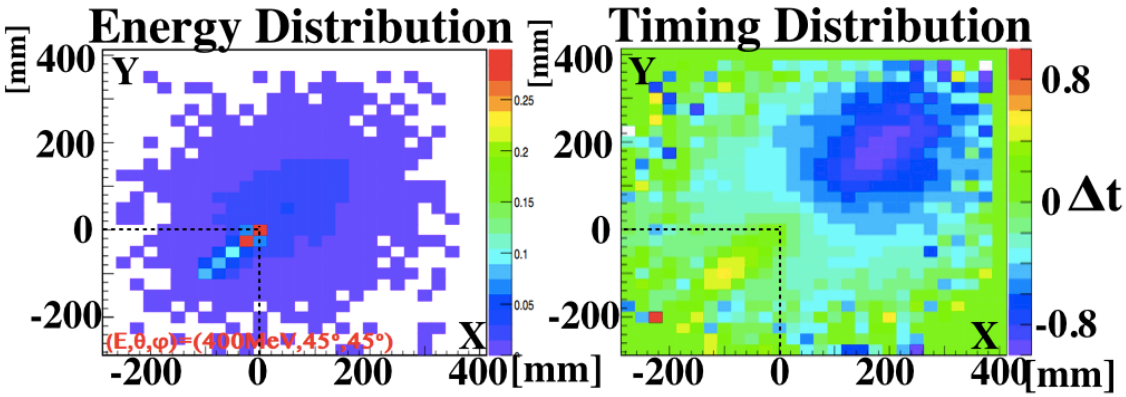

Figure 3. Energy (left) and time difference (right) distributions in a cluster derived from simulation. The X and Y axes show the positions relative to the position with highest energy, and color means energy and time difference.

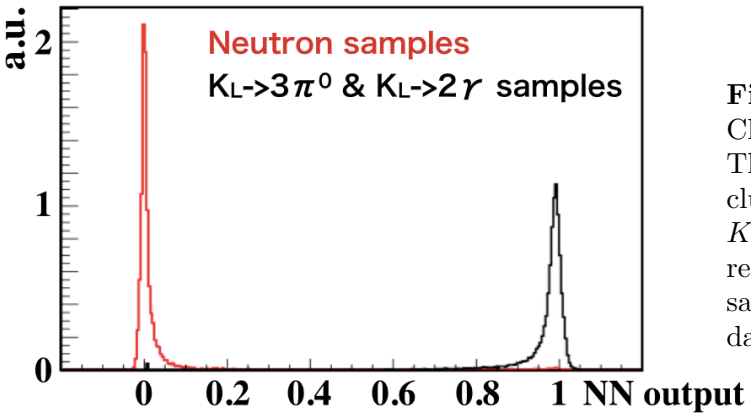

Figure 4. Neural net output of Cluster Shape Discrimination cut. The black histogram shows photon cluster samples obtained by using the $K_L \to 3\pi^0$ and $K_L \to 2\gamma$ modes, and red histogram shows neutron cluster samples obtained using Al target run data.

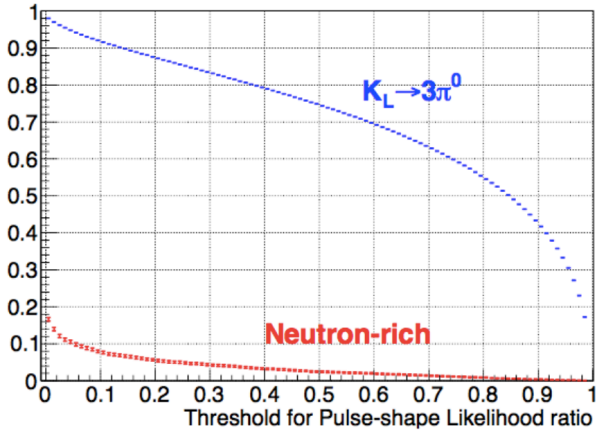

Figure 5. Acceptance of two-photon and neutron-induced events of Pulse Shape Likelihood cut as a function of the likelihood ratio threshold. Blue dots are for the two-photon events derived from $K_L \to 3\pi^0$ samples, and red dots are for the neutron-induced events derived from neutron samples collected in the Al target run.

likely to be a neutron-induced event or a two-photon event. Figure 5 shows the acceptance of two-photon and neutron-induced events as a function of the likelihood ratio threshold. The blue dots are for two-photon events and the red dots are for neutron-induced events. The reduction factor of 10 was obtained with 90% signal acceptance.

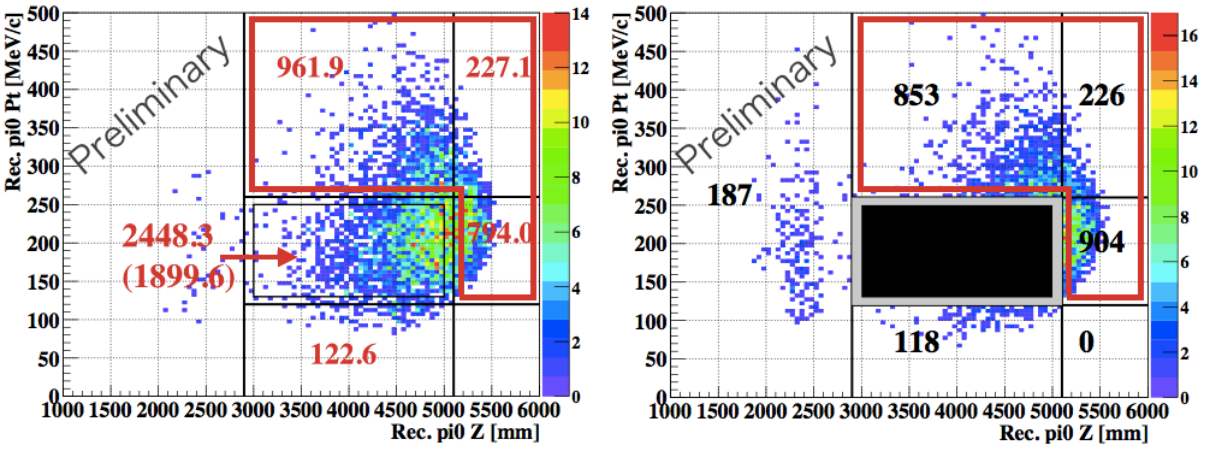

Figure 6. The π^0 P_t v.s. Z scatter plots of the Al target run (left) and the physics run (right) after applying all the cuts except for the neutron cuts. The signal box in the physics plot is blinded. The number "2448.3" in the left figure is the normalized number of events in the box drawn in gray and "1899.6" in parenthesis is the number in the signal box drawn in black.

4. Integration of reduction power of the methods

Both the Shape χ^2 method and the Cluster Shape Discrimination method use the cluster shape information and they are expected to have a strong correlation. The reduction power of these two cuts together was $3.4^{+2.1}_{-0.9} \times 10^3$. The reduction of the Pulse Shape Likelihood was evaluated independently, which was $11.1^{+0.4}_{-0.9}$. The reduction of the Pulse Shape Likelihood with waveform information of individual channels is independent of the reduction from the cluster shape discriminations. [1] The total reduction was obtained as a product of these reduction power , which result in $3.8^{+2.4}_{-1.1} \times 10^4$.

5. Estimation of number of neutron-induced background in physics analysis

In this section, we estimate the number of neutron-induced background events in physics data. The data set used here is 10% of the data taken in 2015. Figure 6 shows π^0 P_t v.s. Z plots for the Al target run and the physics run after applying all the cuts except for the neutron cuts. To estimate the number of neutron-induced background in the physics data, we used the Al target run data. The numbers in black show the number of observed events in each region. To compare the physics and Al target data, the number of events in the Al target run was normalized to the number of events in the physics run data. The normalization factor was calculated by taking the ratio of the number of events in the masked regions to avoid contamination from other background sources. The numbers in red in the Al target run are normalized. After the normalization, we multiply the reduction factor of neutron cuts to the numbers in red.

Figure 7 shows the π^0 P_t versus Z after applying all the neutron cuts. The number of neutron-induced background events in the signal box was estimated to be 0.049.

6. Future prospects : Both-end readout of the calorimeter

To reach the better sensitivity with larger statistics in the future, more reduction power would be needed. We are planning the upgrade of the CsI calorimeter readout.

[1] The Cluster Shape Discrimination uses the timing difference between crystals as an input variable ,which also does not make any correlation to the Pulse Shape Likelihood.

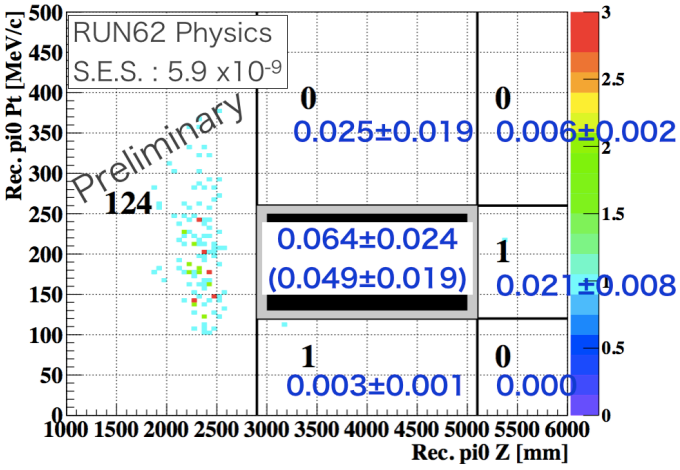

Figure 7. The π^0 P_t versus Z scatter plots of physics run after applying all the cuts including the neutron cuts. The numbers in black show the number of observed events. The numbers in blue show the expected number of neutron-induced background events derived from Al target run data. A number in parenthesis is for the signal box. Only neutron-induced background is considered and contributions from the other background sources are not considered in the estimation.

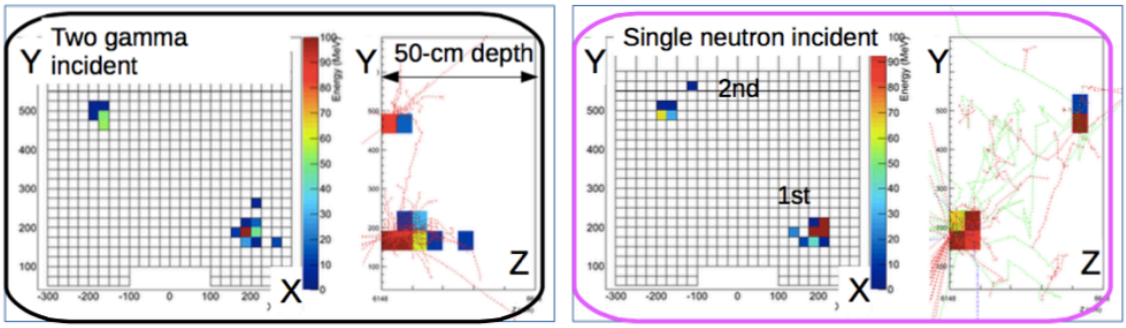

Figure 8. Event displays of a two-photon event (left) and a neutron-induced background event (right) from simulation.

The radiation length of CsI for photons is shorter than the interaction length for neutrons. Thus, if we know the depth of the interaction point, we can distinguish photons from neutrons. Figure 8 shows event displays of a two-photon event and a neutron-induced background event. For photon events, interaction points are in the upstream. Whereas for neutron events, they would distribute broadly. Currently our CsI calorimeter uses PMTs attached downstream-end of the CsI crystals. We plan to add a new photosensor on the upstream-end of the crystals. By using the time difference between the upstream and downstream ends, we would get the Z information of the cluster. A factor of 10 more background reduction is expected by this upgrade. We plan to upgrade the calorimeter in 2018.

7. Conclusion

We have developed several methods to suppress neutron-induced background which is a dominant background in the KOTO experiment. We obtained $(3.8^{+2.4}_{-1.1}) \times 10^4$ reduction power for this background and number of background events was estimated to be 0.049 for the data corresponding to the single event sensitivity of 5.9×10^{-9}.

We also have a plan to upgrade our CsI calorimeter readout. The new both-end readout system will give us a factor of 10 more background reduction. This upgrade is planned to be made in 2018.

References

[1] A. J. Buras, D. Buttazzo, J. Girrbach-Noe and R. Knegjens, *J. High Energy Phys.* **1511**, 033 (2015).
[2] J.K. Ahn *et al.*, arXiv:1609.03637 [hep-ex].
[3] J. K. Ahn *et al.*, *Phys. Rev.* **D** 81, 072004 (2010).